Fluorescence Probing of Inverted Micelles. The State of Solubilized Water Clusters in Alkane/Diisooctyl Sulfosuccinate (Aerosol OT) Solution

M. Wong,[1a] J. K. Thomas,*[1a] and M. Grätzel[1b]

Contribution from the Radiation Laboratory and Chemistry Department, University of Notre Dame, Notre Dame, Indiana 46556, and the Hahn-Meitner-Institut für Kernforschung Berlin GmbH, Bereich Strahlenchemie, 1 Berlin 39, West Germany.
Received August 26, 1975

Abstract: The nature of the aqueous core of inverted micelles was tested by fluorescence techniques. The emission properties of 1,8-anilinonaphthalenesulfonate (ANS) were found to be extremely sensitive to the size of solubilized water clusters. The fluorescence yield and lifetime decrease with increasing radius of the aqueous core while the position of the emission maximum shifts to longer wavelengths. The microviscosity of the interior of AOT micelles was examined by fluorescence polarization experiments. The emission of rhodamine B is strongly polarized in the absence of water indicating a very rigid structure of the micellar core. The microviscosity decreases with increasing size of the solubilized water cluster. The dynamics of motion of cationic (Cu^{2+}, Tl^{+}) and nonionic species within the inverted micellar core were examined using time correlated fluorescence and laser photolysis techniques. The kinetics of pyrenesulfonic acid fluorescence in the presence of these quenchers show that the motion of the ionic quenchers is very restricted at small H_2O cluster size. On the other hand, O_2 can undergo unrestricted diffusion. The fluorescence observations are explained in terms of Na^{+} dipolar interactions leading to rigid structures of the aqueous micellar core at small H_2O/Na^{+} ratios.

Although the physical nature of synthetic micelles in aqueous solution has been extensively investigated, relatively little information is presently available about the static and dynamic properties of inverted micelles. The latter aggregates are present in solutions of various amphiphiles in nonpolar organic solvents.[3] Their structure is such that the polar head groups of the amphiphiles constitute the core of the aggregate while the hydrophobic tails extend into the surrounding solution. Among these amphiphiles capable of forming inverted micelles diisooctylsodium sulfosuccinate (Aerosol OT, AOT) has received particular attention.[4] The interest focuses on the ability of AOT micelles to solubilize relatively large amounts of water in a variety of hydrophobic organic liquids.[5] The water is accommodated in the polar centers of the aggregates where it forms spherical pools the sizes of which are controlled by the AOT/H_2O ratios.[6a] Investigations of inverted micelles containing solubilized water clusters seem attractive for two reasons.

(i) These systems have considerable industrial importance. For example, AOT/H_2O/chloroethylene mixtures are used in the dry-cleaning process.[6b]

(ii) Addition of H_2O to AOT alkane solutions produces molecular organization similar to pockets of water in bioaggregates (biomembranes, mitochondria,[7] etc.). Some pertinent physical features of such aqueous microphases in a hydrophobic environment may be explored by means of micellar model systems. AOT/H_2O micelles are a suitable choice for these investigations since they are well defined with respect to size, shape, and aggregation number.

The aqueous microphase located in the interior of inverted AOT micelles has already been characterized with respect to NMR,[5b,c] ir resonance frequencies,[4b] specific volume,[6a] and solubility of electrolyte.[6b] These parameters were all found to be different from those of bulk water indicating strong interaction of water dipoles with sodium counterions and ionized succinate headgroups. Similar conclusions have been reached from ESR spin probe analysis[8] and kinetic studies of ester hydrolysis in water pools.[9] The present study utilizes the advantages of the technique of fluorescence probing to gain further insight into the nature of the polar cavities in the interior of AOT micelles. These investigations parallel earlier work where similar techniques were applied to the study of micelles in aqueous solution.[10] 1,8-Anilinonaphthalenesulfonate (ANS), pyrenesulfonic acid (PSA), and rhodamine B were selected as fluorescent probes. In AOT/alkane solutions all these probes display a strong affinity for the polar core of inverted AOT micelles.

The properties of ANS fluorescence, e.g., quantum yield, lifetime, and position of the fluorescence maximum, are extremely sensitive to the polarity of the microenvironment.[11] This behavior may be used to test the effective polarity of the AOT micellar core in the absence and presence of water on the other hand. PSA has a comparatively long fluorescence lifetime. Hence, from the time sequence of PSA fluorescence and the kinetics of quenching reactions the dynamics of motion of PSA and quencher ions inside the AOT micelles can be inferred. Finally, rhodamine B is suitable for fluorescence polarization studies. These data give information about the microviscosity within the AOT micelles.

Experimental Section

Materials. Di(2-ethylhexyl)sodium sulfosuccinate (Aerosol OT), 100%, was a generous gift from American Cyanamid Corp. For further purification the material was dissolved in methanol and the solution was filtered, a residual white residue being discarded. The solvent was then evaporated under vacuum. A white precipitate was obtained which was dried under vacuum at 40 °C for 1 day. The purified AOT sample was stored in a vacuum desiccator over P_2O_5. 1,8-Anilinonaphthalenesulfonate (K & K Laboratories) was purified by repeated recrystallization from aqueous saturated $MgCl_2$ solutions using Norit as a decolorizing agent. Water was first distilled from a Barnsted still and subsequently from alkaline permanganate. Pyrenesulfonic acid (Pfaltz and Bauer), rhodamine B (Allied Chemicals), heptane, and dodecane (Phillips 66, research grade) were used as supplied.

Sample Preparation. Water was solubilized in the AOT/alkane solutions by stirring the mixture at room temperature for ca. 20 min. The AOT concentration was maintained at 3% w/v throughout the work. All experiments were performed with freshly prepared solutions. Oxygen was removed from most of the samples by flushing with nitrogen. Care had to be taken not to evaporate water during this procedure.

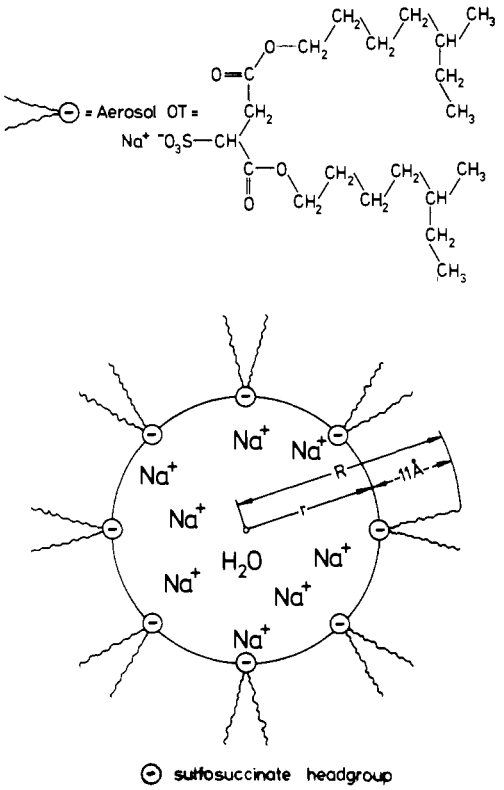

Figure 1. Schematic illustration of an AOT inverted micelle with an aqueous core.

Apparatus. Static fluorescence measurements were carried out with an Aminco-Bowman spectrofluorometer. A thermocouple inserted in the fluorescence cell was used to monitor the temperature of the solutions. The temperature was adjusted by means of a thermostated cell holder which was supplied with water or cooled nitrogen gas. A polarization attachment was used for polarized fluorescence experiments. A detailed description of this technique has been given elsewhere.[12] Laser photolysis experiments were carried out with a frequency doubled K1QP Korad ruby laser. The outputs in the 694.2- and 347.1-nm lines were 2 J and 100 mJ, respectively. The duration of the pulse was 15 ns. The time sequence of the fluorescence after laser excitation was observed by fast kinetic spectroscopy.[13] (A 0.3-ns cerenkov light pulse was used to excite fluorophores.) When measuring very fast fluorescence events the cerenkov light was produced by irradiating a quartz target with a 0.3-ns electron pulse from a Van de Graaff accelerator. The subsequent fluorescence was recorded with an oscilloscope–photomultiplier system which had a rise time of 0.5 ns.

Determination of Absolute Quantum Yield. Absolute fluorescence quantum yields were determined for ANS in AOT/H_2O/heptane solutions by comparing the area underneath the emission-wavelength curve A_H with the corresponding area A_M obtained from an ANS/methanol solution. As the fluorescence curves of both solutions were measured under identical conditions (temperature, ANS concentration, geometry), the quantum yield in the micellar system is related to the known quantum yield in methanol by

$$\phi_H = \phi_M(1 - T)_M A_H n_M^2/(1 - T)_H A_M n_H^2$$

where n_M and n_H denote the refractive index of methanol and AOT/H_2O/heptane, respectively. T is a geometric parameter which is approximately 0 for a fluorescence detection device with large separation of phototube and sample cell.

Results and Discussion

In a 3% solution of AOT in heptane or dodecane the AOT molecules are completely associated in uniformly sized assemblies, each consisting of 23 AOT molecules. The structure of such an aggregate is slightly asymmetric and may be best represented by a rounded cylinder with a rod length of 33.4 Å and a cylindrical diameter of 23.9 Å.[4b] The degree of asymmetry is greatly reduced in the presence of water which forms a spherical pool in the micellar center. The aqueous core is surrounded by a monolayer of AOT molecule resulting in the configuration shown by Figure 1. The total micellar radius R is composed of the length of an AOT molecule (=11 Å) and the radius of the water pool which can be calculated from

$$r(\text{Å}) = 36.65v/g^5 \qquad (1)$$

where v and g are the weight percentages of water and AOT, respectively. The validity of eq 1 has been verified by ultracentrifugal and light-scattering measurements. Table I lists R values and micellar compositions for relevant AOT solutions used in our experiments.

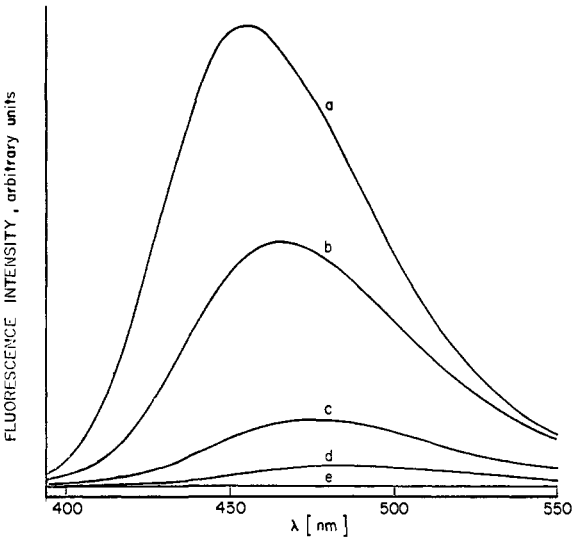

Figure 2. Effect of H_2O on the fluorescence spectrum of ANS (4×10^{-6} M) in AOT/H_2O/heptane solutions; excitation wavelength 360 nm; water content (%) (a) 0, (b) 0.2, (c) 0.5, (d) 2, (e) 6.

Table I. Micellar Composition[a] and Dimensions[b] for AOT Solutions Employed in the Experiments

%(v/v) of H_2O	6	2	1	0.5	0.2
N_{H_2O}/N_{AOT}	493	16.4	8.2	4.1	1.64
N_{H_2O}/micelle	552 570	20 465	2558	319	21
R, Å	84	35.4	23.2	17.1	13.4

[a] AOT content: 3% (w/v). [b] Calculated from eq 1.

Behavior of ANS Fluorescence

Steady state fluorescence spectra measured at different water concentrations in AOT/H_2O/heptane solutions are shown in Figure 2. The gross features of these curves have already been discussed in a previous communication.[14] In water-free AOT solution ANS displays very intense fluorescence which appears as a broad structureless band with maximum intensity at λ_{max} 450 nm. This fluorescence is drastically quenched by the addition of water with a concomitant red shift of λ_{max}. Similar behavior is exhibited by ANS in dodecane/AOT solutions as is shown by Figure 3. Separate plots of fluorescence quantum yields as well as λ_{max} values vs. the H_2O concentration are presented in Figures 4 and 5. It is apparent that the changes in the latter parameters are most significant in a region where the water content of the micelles is relatively small, and approaches a plateau at larger radii of the water pools.

Figure 6 demonstrates the influence of H_2O on the time course of the ANS emission. The τ_F values obtained are 10, 6, and 2.5 ns in AOT/heptane solutions containing 0, 0.2,

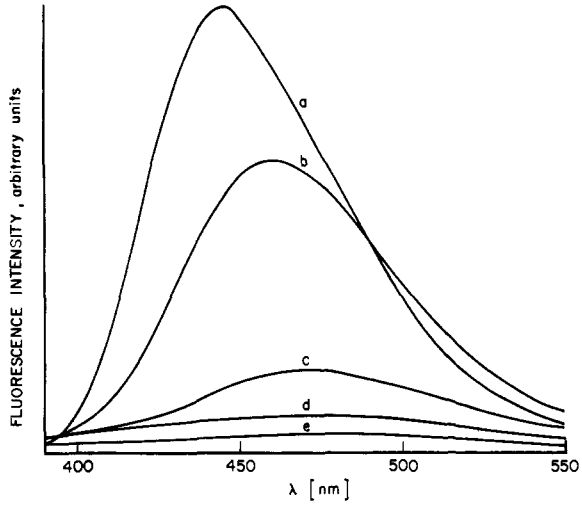

Figure 3. Effect of H_2O on the ANS fluorescence spectrum in AOT/H_2O/dodecane solutions; conditions as in Figure 2. Water content (%) (a) 0, (b) 2, (c) 5, (d) 1, (e) 2.

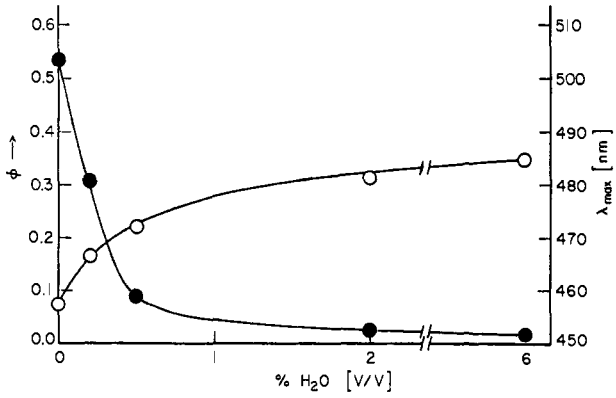

Figure 4. Quantum yield and maximum wavelength of ANS fluorescence vs. H_2O concentration in AOT/heptane.

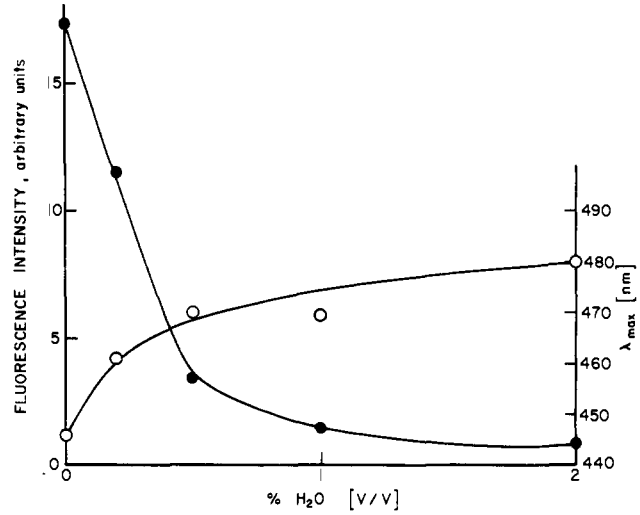

Figure 5. Quantum yield and maximum wavelength of ANS fluorescence vs. H_2O concentration in AOT/dodecane.

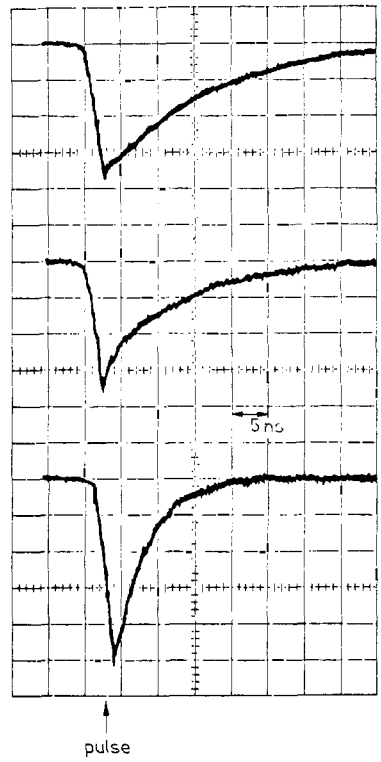

Figure 6. Oscilloscope traces showing the effect of water on ANS fluorescence decay kinetics in AOT/heptane: [ANS] = 5×10^{-6} M, from the top [H_2O] = 0, 0.2, 0.5%.

and 0.5% H_2O, respectively. This behavior shows that ANS fluorescence quenching by H_2O is an efficient and dynamic process.

Practically no fluorescence was observed with 2×10^{-6} M ANS in pure heptane or dodecane indicating that the presence of AOT inverted micelles is required to produce the very intense emission. This shows that ANS is similar to other ionic dyes[15] and is incorporated into the core of AOT inverted micelles. The ANS fluorescence properties may then be exploited to derive information about the discrete microenvironment of the AOT micellar interior.

The fluorescence behavior of ANS in various media has been investigated extensively.[11,16] In particular, ANS fluorescence probes have been widely employed as polarity indicators in biological systems. A more polar environment leads to smaller quantum yields and red shift of the emission. Recently a detailed report on the photophysical events occurring during ANS irradiation has been published.[17] According to this study ANS excitation leads to formation of S_I excited singlet state which subsequently can undergo intramolecular charge transfer to form another excited singlet state $S_{I,CT}$. Emission can occur from both states. Solvents of high polarity promote the charge-transfer transition $S_I \rightarrow S_{I,CT}$ and the rate of radiative deactivation of $S_{I,CT}$, and decrease the frequency of the $S_{I,CT} \rightarrow S_0$ fluorescence. However, the rates of the two processes, $S_I \rightarrow S_{I,CT}$ and $S_{I,CT} \rightarrow S_0$, are controlled not only by the polarity of the medium but also by the viscosity in the environment of the probe.

It seems reasonable then to explain the data in Figures 2 to 6 in terms of variations in the effective polarity and viscosity of the micellar interior with the size of the incorporated water pockets. The quantum yield and λ_{max} value obtained with water-free AOT solutions are comparable to those in dioxane indicating the similar nature of the two media. The polarity increases as water is incorporated into the micelles. However, the fluorescence yield and spectral maximum obtained with the largest water cluster (ϕ = 0.018; λ_{max} 484 nm) are still considerably greater than the respective parameters of bulk water (ϕ = 0.0038; λ_{max} 510 nm).[16c] This indicates that the effective polarity of a pool with a radius as large as 70 Å incorporated into AOT in-

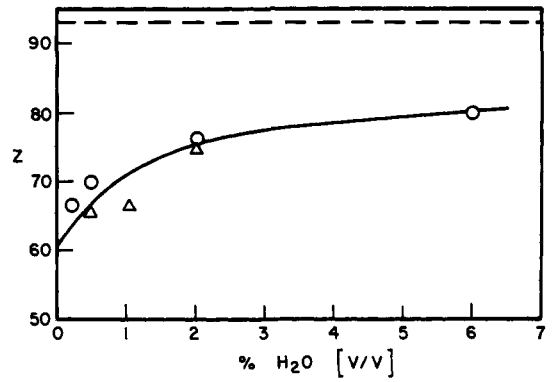

Figure 7. Kosower's Z value evaluated from ANS fluorescence results vs. H_2O concentration in AOT/alkane solutions: (△) dodecane, (○) heptane.

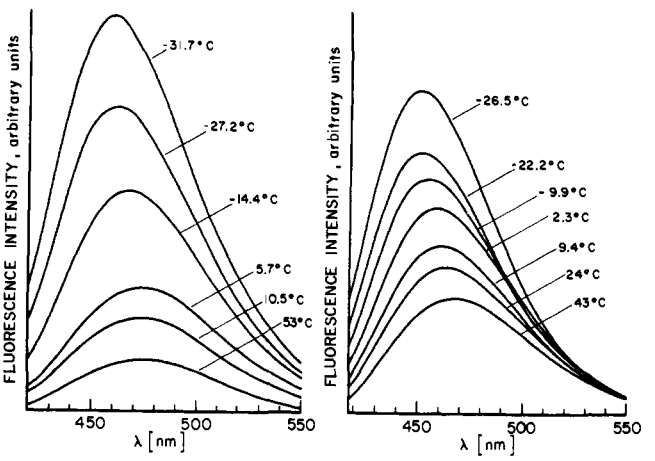

Figure 8. Temperature effect on ANS fluorescence curves: [ANS] = 4×10^{-6} M; (left) AOT/0.5% H_2O/heptane; (right) AOT/0.2% H_2O/heptane.

verted micelles is smaller than that of an aqueous bulk phase.

While it is difficult to relate ANS fluorescence properties to an exact macroscopic measurement of the polarity such as dielectric constant and refractive index, nevertheless a close correlation exists with the empirical Z solvent polarity scale of Kosower.[18] In particular, it has been shown that Z values and the relative positions of ANS fluorescence and absorption maxima are interconnected.[16e] Applying this concept to the data in Figures 4 and 5, one obtains Z values for the interior of inverted micelles in the absence or presence of solubilized water. The results which are presented in Figure 7 again indicate an increase in polarity with increasing size of the water clusters, the Z value for the larger pool remaining well below that of bulk water.

The drastic changes in the ANS fluorescence parameters occurring at small H_2O:AOT molar ratios may profitably be discussed more fully at this point. For a correct interpretation of these effects a consideration of the intermolecular forces prevailing within the water pools is required. The ion dipole attraction between sodium counterions and solubilized H_2O plays a prominent role. The Na^+-H_2O interaction energy is of the order of 25 kcal/mol H_2O.[19] Hence it is anticipated that water is bound extremely firmly up to the completion of the Na^+ hydration shell, i.e., $[H_2O]/[Na^+] = 6$. Water which is not used for hydration can still undergo binding by ion dipole forces or via hydrogen bonds to sulfonate or carboxyl groups present in the cavity. Although these interactions are much weaker than the attractive forces between Na^+ and H_2O they nevertheless engage water molecules up to a ratio $[H_2O]/[AOT] = 12$. Only water in excess of this limit can be regarded as comparably free with the properties of a true dispersion medium.[4a] Applying these considerations to the ANS fluorescence data one realizes that the sharp increase in ϕ_F and the concomitant decrease of λ_{max} occurs precisely at a point where the water content of the micelles falls below the ratio $[H_2O]/[Na^+] = 6$. Evidently water participating in Na^+ hydration cannot rotate as freely as bulk water. This increases the microviscosity in the micellar core and hence decreases the rates of the $S_1 \rightarrow S_{1,CT}$ intramolecular charge transfer. Under such conditions the S_1 emission will dominate over that from S_{CT} states and therefore the fluorescence will occur at shorter wavelengths and with much higher quantum yields.

The effect of water immobilization by Na^+ counterions may be illustrated further by examining the influence of temperature on the ANS fluorescence behavior. Figure 8 shows ANS emission curves obtained from solutions of 4×10^{-6} M ANS in 3% AOT containing 0.2 and 0.5% H_2O. Within the temperature range examined (+50 to −30 °C) the fluorescence quantum yield increases strongly with decreasing temperature and the position of the fluorescence band shifts toward the blue. The augmentation of ϕ_F is attributed to a decreased rate constant for the nonradiative deactivation process of ANS singlet excited states as the temperature coefficient of the radiative rate constant k_r is relatively small. The main pathway of radiative deactivation can be sought in formation of $S_{1,CT}$ ANS excited states via intramolecular charge transfer. Hence it seems reasonable to conclude that the very intense and blue-shifted fluorescence observed at lower temperatures originates mainly from S_1 states. The processes $S_1 \rightarrow S_{1,CT}$ and the radiationless deactivation of $S_{1,CT}$ are both charge-transfer reactions and involve rotational motion of H_2O dipoles about ANS fluorophores as well as rotation of the aromatic rings within an ANS molecule.[17] Thus it is concluded that the temperature effect on ϕ_F and λ_{max} mainly reflects changes in the rotational freedom of H_2O molecules adjacent to the excited probe.

It is particularly instructive to examine the influence of temperature on the position of the ANS emission maximum in more detail. Figure 9 shows λ_{max}-(T) plots for three different sizes of water clusters. In the case of the AOT/heptane solution with the largest water content (2%) the shift of the λ_{max} in the temperature range $0 < T < 30$ °C is relatively small. The gradient $\Delta\lambda_{max}/\Delta T$ becomes large only after the temperature decreases below the freezing point. This indicates relatively free motions of H_2O dipoles at $T > 0$ °C and strongly restricted motions at $T > 0$ °C where ice-like structures may be present in the water pools. The gradient of λ_{max} at room temperature increases with decreasing size of the water clusters, and becomes particularly steep at a point where the water content of the micelle falls below the ratio $[H_2O]/[Na^+] = 6$. Such behavior can be explained in terms of a larger activation energy for the rotational correlation time of the water as compared to that of free water.

It is concluded from the ANS fluorescence analysis that the parameters ϕ_F and λ_{max} are related to the micropolarity of the AOT micellar core only at relatively large $[H_2O]/[Na^+]$ ratios. In smaller clusters the dynamics of H_2O dipolar rotation rather than local polarity determine these ANS fluorescence properties. These results have bearing on the wide use of ANS as a probe for the polarity of specific sites of biological aggregates. It is obvious that ANS can function reliably as a polarity indicator only under conditions where intramolecular charge transfer subsequent to excitation of the probe is faster than emission from unrelaxed S_1 states.

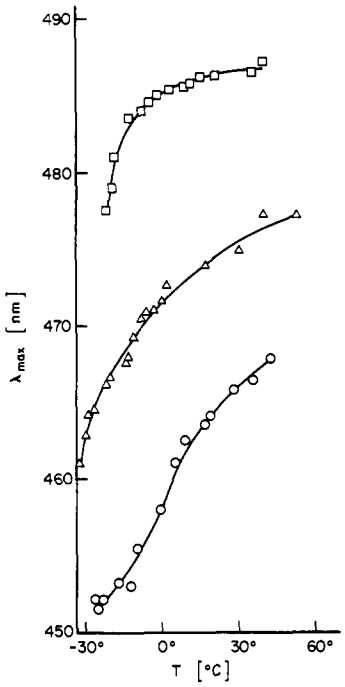

Figure 9. Position of the fluorescence maximum of ANS vs. temperature: (○) 2% H_2O; (△) 0.5% H_2O; (□) 2.0% H_2O (v/v).

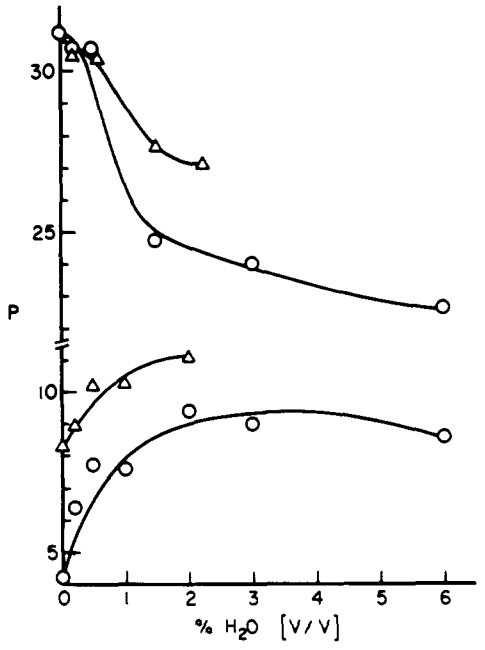

Figure 10. Effect of H_2O on the degree of fluorescence polarization in AOT/alkane solution. Lower curves, ANS (4×10^{-6} M), λ_{exc} 546 nm: (△) dodecane, (○) heptane.

Fluorescence Polarization Measurements

The degree of polarization of the fluorescence emitted from a probe molecule can serve as a measure for the local viscosity in the vicinity of the fluorophore. The application of this technique to the study of bioaggregates has been reviewed.[11b] The relation between the degree of polarization P and the microviscosity is given by Perrin's equation,

$$(1/P - 1/3)/(1/P_0 - 1/3) = 1 + kT\tau_F/\eta V_0 \qquad (2)$$

where the symbols are defined as follows: P_0 is the fluorescence polarization in a solvent of extremely high viscosity; τ_F is the lifetime of the fluorescent excited state; T is the temperature in °K; k is Boltzmann's constant; V_0 is the effective volume of the fluorescent molecule.

The polarizations of the fluorescence of two ionic dyes, rhodamine B and ANS, were analyzed in alkane solutions of AOT inverted micelles and the results are displayed in Figure 10. With rhodamine B a P value of 0.32 was obtained in water-free solutions indicating the highly polarized character of the emission. (The theoretical limit P_0 is 0.45 at the applied excitation wavelength.) Depolarization of light emitted from probes that are associated with micelles can originate from two different rotational processes: movement of the probe within the micelle and rotation of the micelle as a whole. A decrease of P from 0.45 to 0.32 can be accounted for by the second process. Hence it is concluded that rhodamine B is held in an extremely rigid microenvironment which does not allow rotation of the fluorophore within the inverted micelle during the lifetime of the excited state. Similar effects have been observed with other types of inverted micelles and have been utilized to determine the volumes of these aggregates.[15]

Addition of water causes a substantial decrease in the degree of polarization of rhodamine B fluorescence. Perrin's equation predicts that variations of P may result from a change in the fluorescence lifetime τ_F or the microviscosity η. The first possibility can be ruled out on the basis of fluorescence yield measurements performed with rhodamine B/AOT/H_2O solution. As ϕ_F was hardly affected by the addition of water it is expected that τ_F remains approximately constant within the investigated H_2O range. Therefore the observed decrease in P is attributed to an augmentation of the degree of fluidity leading to greater freedom of movement for the incorporated fluorophore with increasing size of the solubilized water pool. It should be noted that the addition of water drastically enlarges the volume and aggregation number of AOT micelles and consequently decreases the contribution of the micellar rotation to the overall depolarization. This effect tends to offset the decrease in P caused by the gain in rotational freedom of the probe at higher water concentrations. Hence the augmentation of fluidity within the aqueous micellar core upon addition of H_2O is actually larger than indicated by the change in the degree of polarization. Inspection of the P vs. (% H_2O) curves for rhodamine B shows, furthermore, that the slopes are steepest at a point where the water concentration falls below 1%, This behavior reflects a strong increase in microviscosity of the micellar interior when the amount of solubilized H_2O approaches the limit for Na^+ counterion solvation. Thus, the rhodamine B fluorescence polarization analysis amplifies the earlier conclusions concerning the nature of the water clusters incorporated in AOT micelles, in particular, the importance of Na^+–H_2O interaction for the motility of solubilized H_2O molecules.

The features of the polarization curves for ANS fluorescence in Figure 10 differ conspicuously from those for rhodamine B. In the absence of water the P values in AOT/dodecane and AOT/heptane solutions are only 8 and 4%, respectively. In contrast to rhodamine B solutions the polarization increases upon addition of water until it reaches a plateau, and only at the largest accessible water concentration is a slight decrease in P noticeable. A major reason for this behavior may be sought in the drastic effect exerted by H_2O on the ANS fluorescence lifetime. It was shown in the preceding chapter that water sharply enhances the decay rate of ANS excited states. At small cluster sizes this effect apparently dominates over the decrease in microviscosity. Hence the ratio τ_F/η decreases as the amount of solubilized water becomes larger; this leads to the observed increase in P (eq 2). In the plateau region changes in τ_F and η seem to balance and P remains approximately constant.

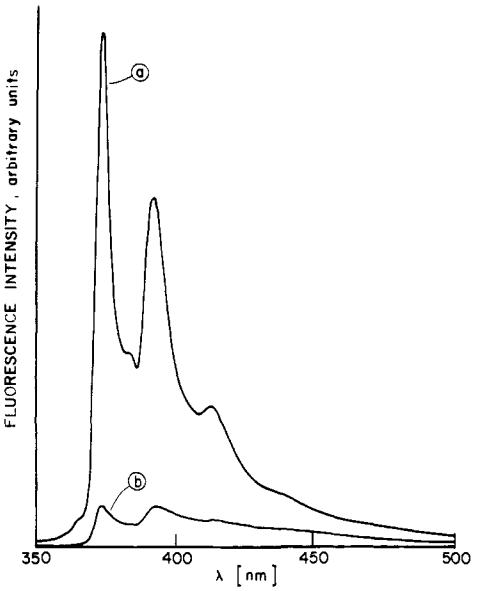

Figure 11. Fluorescence spectra of pyrenesulfonic acid (2×10^{-5} M) in AOT/H_2O/heptane solution ([H_2O] = 3%): upper curve deaerated, lower curve aerated.

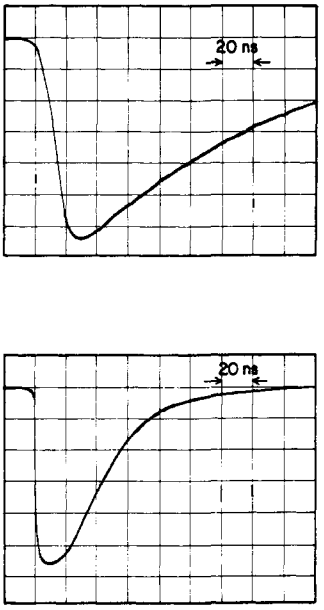

Figure 12. Oscilloscope traces of the PSA fluorescence decay at 400 nm after 347.1-nm laser excitation; conditions as in Figure 11. Upper curve, deaerated; lower curve, aerated.

A further point which has to be considered when comparing ANS and rhodamine B fluorescence polarization is the respective sites of solubilization in the inverted AOT micelle. Rhodamine B is a cation and, therefore, is expected to associate with anionic succinate head groups, the aromatic moiety protruding into the AOT hydrophobic tails. Conversely, as ANS is negatively charged it is repelled from the surface and its favored location is the aqueous micellar interior. This region may be more fluid in nature than the boundary between aqueous and hydrocarbon phase where ice-like water structure could prevail. This could explain the differences in P observed for the two probes at the larger water cluster sizes. Finally, the difference between ANS fluorescence polarization in water-free heptane and dodecane is attributed to the effect of solvent viscosity on the rate of micellar rotation. Depolarization of fluorescence by

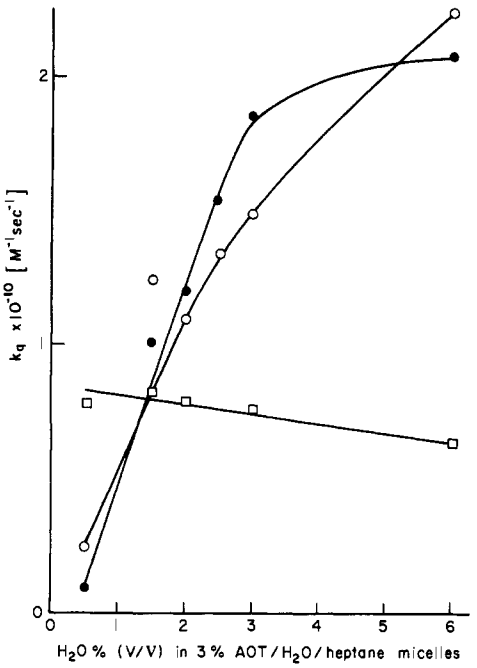

Figure 13. Effect of water on the specific quenching rates of PSA fluorescence by (○) Cu^{2+}, (●) Tl^+, (□) O_2 in AOT/H_2O/heptane solution. The curve for O_2 was offset (see text).

this process is expected to occur to a greater extent for ANS than in the case of rhodamine B, as the τ_F value for the former probe (=10 ns) is much longer than that for the latter (<1 ns). The viscosity of dodecane is greater than that of heptane, hence the larger degree of fluorescence polarization.

The above discussion has centered around the statement that PSA and ANS are primarily in the water core of the micelle. It is possible that these molecules tend to reside in the hydrocarbon tails of the micelle. The effect of water content on the ANS fluorescence is thus decreased. Such a situation also affords a ready explanation for the O_2 quenching data in a subsequent section. Further experiments with more hydrophillic probes are required to elucidate the precise situation.

Steady State Fluorescence and Laser Fluorescence and Laser Photolysis Experiments with Solutions of PSA in Inverted AOT Micelles

The fluorescence spectrum of PSA in water and aqueous micellar solution has been previously reported.[20] PSA is very insoluble in solvents such as heptane or dodecane, and these solutions display only very weak fluorescence. However, PSA is readily incorporated into AOT inverted micelles. These solutions are strongly fluorescent and the spectral features of the steady state emission are shown in Figure 11. The spectrum resembles that of PSA in aqueous solution. Three peaks with maxima at λ 373, 382, and 414 nm are observed which are characteristic for the pyrene fluorophore and correspond to vibrational fine structure of the S_1-S_0 transition. Unlike ANS the quantum yield of PSA fluorescence is only slightly affected by addition of water to the system. However, as shown in the figure, the emission is strongly quenched by oxygen.

The dynamics of PSA fluorescence in inverted AOT micelles were examined by laser photolysis technique using fast optical methods to monitor the time sequence of the emission. Typical oscilloscope traces showing the fluorescence decay in deaerated and aerated AOT/H_2O/heptane solutions are presented in Figure 12. The decay curves obey

first order kinetics and τ_F values of 122 and 18 ns are obtained from semilog plots of the two curves. The size of the aqueous core of AOT micelles has only a modest effect on the PSA fluorescence lifetime. The τ_F values decrease from 144 ns in H_2O-free solution to 100 ns for the largest accessible water concentration of 6%. Even under the latter conditions the lifetime is still considerably longer than in pure aqueous solution,[20c] a result which again stresses the difference in the properties of such a large water cluster from that of bulk water.

The drastic shortening of τ_F induced by oxygen confirms the observation of very small fluorescence quantum yields in aerated solutions (Figure 11). The time-resolved fluorescence demonstrates, moreover, that the quenching action is a dynamic process involving diffusion of the perturber toward the PSA probe. The bimolecular rate constant for such a quenching reaction is given by the expression

$$k = 1/[Q](1/\tau_F - 1/\tau_F^0) \quad (3)$$

where [Q] denotes the quencher concentration and τ_F and τ_F^0 are the fluorescence lifetimes in the presence and absence of quencher. A rate constant $k_q = 9 \times 10^{10}$ M^{-1} s^{-1} is obtained when the solubility coefficient for oxygen in pure water is used to calculate [Q] in eq 3. This value seems unusually high as it is considerably larger than the limit for the rate of a diffusion-controlled reaction. A more reasonable k_q value of 7.5×10^9 M^{-1} s^{-1} as derived from eq 3 if the O_2 concentration in heptane is inserted for [Q]. From these results it seems unlikely that only O_2 present in the aqueous micellar core can participate in the quenching reaction. Rather, it must be concluded that this process involves also oxygen from the hydrocarbon bulk phase which, apparently, can readily enter the micelle. An attempt was made to measure the effective O_2 content in the water bubble by the reaction of a hydrated electron e_{aq}^- with O_2. In free water the rate constant for this reaction is 2×10^{10} M^{-1} s^{-1}. Hydrated electrons were generated in the inverted micelles, in the presence and absence of O_2, by pulse radiolysis and the rate of decay of e_{aq}^- observed. The measured rate of decay of e_{aq}^- in the presence of O_2 together with the rate constant of 2×10^{10} M^{-1} s^{-1} gives an effective $[O_2]$ in aerated micelles of 5.5×10^{-4} M/l. Hence this $[O_2]$ gives a $k_{PSA^*+O_2}$ of 4.55×10^{10} M^{-1} s^{-1} which is closer to the diffusion limit of 2×10^{10} M^{-1} s^{-1}.

As indicated in an earlier section the range O_2 quenching constant can be explained if PSA resides toward the hydrocarbon phase where the O_2 concentration is larger than in the micellar water core.

Figure 13 shows the influence of H_2O concentration on the PSA fluorescence quenching rate for O_2, Cu^{2+}, and Tl^+ ions. In pure aqueous phase the k_q parameters for these species are around 2×10^{10} M^{-1} s^{-1} which indicates diffusion-controlled reaction with PSA excited states. It is instructive to juxtapose the quenching results for O_2 and the cationic quenchers in AOT inverted micelles. Apparently k_q for oxygen is almost independent of H_2O concentration indicating that O_2 can diffuse with great ease toward the site of the fluorophore, even in smaller water clusters where the microviscosity is very high. Conversely, the size of the aqueous micellar core drastically affects the k_q parameters of the cationic quenchers. In a solution containing 6% H_2O (core radius 72 Å) their quenching efficiency is high reflecting relatively unrestricted motion of the solubilized quencher ions. The k_q values decrease markedly as the core radius decreases, the effect becoming most pronounced at $[H_2O]$ = 2%. These observations indicate that the movement of the quencher ion is retarded as the size of the water cluster decreases, and prevented almost completely under conditions where the water content of the micelle is merely sufficient for solvation of ionic species inside the aqueous core.

Conclusion

This paper illustrates photochemical data that give a measure of the nature of water in the core of inverted micelles of AOT in hydrocarbons. Preliminary kinetic measurements indicate that the water composition plays a significant role in the simple reactions studied. Further kinetic experiments are designed to investigate these systems in further detail.

Acknowledgment. Acknowledgment is made to the donors of the Petroleum Research Fund, administered by the American Chemical Society, for partial support of this research.

References and Notes

(1) (a) University of Notre Dame; (b) Hahn-Meitner-Institut für Kernforschung Berlin GmbH.
(2) The Radiation Laboratory of the University of Notre Dame is operated under contract with the U.S. Energy Research and Development Administration. This is ERDA Document No. COO-38-1008.
(3) (a) P. A. Winsor, *Chem. Rev.*, **68**, 1 (1968); (b) C. Singleterry, *J. Am. Oil Chem. Soc.*, **32**, 446 (1955); (c) P. H. Elworthy, A. T. Florence, and C. B. MacFarlane, "Solubilization by Surface Active Agents", Chapman and Hall Ltd., London, 1968.
(4) (a) J. B. Peri, *J. Am. Oil Chem. Soc.*, **35**, 110 (1958); (b) P. Ekwall, L. Mandell, and K. Fontell, *J. Colloid Interface Sci.*, **33**, 215 (1970); (c) W. J. Knox and T. O. Parshall, *ibid.*, **40**, 290 (1972); (d) A. Kitahara, T. Kobayashi, and T. Tochibana, *J. Phys. Chem.*, **66**, 363 (1962).
(5) (a) W. I. Higashi and J. Misra, *J. Pharm. Sci.*, **51**, 455 (1962); (b) S. G. Frank, Y. H. Shaw, and N. C. Li, *J. Phys. Chem.*, **77**, 239 (1973); (c) S. G. Frank and G. Zografi, *J. Colloid Interface Sci.*, **23**, 243 (1967).
(6) (a) M. B. Mathews and E. J. Hirschhorn, *J. Colloid Sci.*, **8**, 86 (1953); (b) C. M. Aebi and J. R. Wiebush, *ibid.*, **14**, 101 (1959).
(7) B. Chance, *Proc. Natl. Acad. Sci. U.S.A.*, **67**, 560 (1970).
(8) F. M. Menger, G. Saito, G. V. Sanzero, and J. R. Dodd, *J. Am. Chem. Soc.*, **97**, 909 (1975).
(9) F. M. Menger, J. A. Donohue, and R. F. Williams, *J. Am. Chem. Soc.*, **95**, 286 (1973).
(10) M. Grätzel and J. K. Thomas, "Modern Fluorescence Spectroscopy", E. L. Wehry, Ed., Plenum Press, New York, N.Y., in press.
(11) (a) G. Weber and D. J. R. Laurence, *Biochem. J.*, **56**, 31 (1954); (b) G. Weber, *Ann. Rev. Biophys. Bioeng.*, **1**, 553 (1972).
(12) M. Grätzel and J. K. Thomas, *J. Am. Chem. Soc.*, **95**, 6885 (1973).
(13) R. McNeil, J. T. Richards, and J. K. Thomas, *J. Phys. Chem.*, **74**, 2290 (1970).
(14) M. Wong, M. Grätzel, and J. K. Thomas, *Chem. Phys. Lett.*, **30**, 329 (1975).
(15) (a) L. Arkin and C. R. Singleterry, *J. Am. Chem. Soc.*, **70**, 3965 (1948); (b) L. Arkin and C. R. Singleterry, *J. Colloid Sci.*, **4**, 537 (1949); (c) C. R. Singleterry and L. Arkin-Weinberger, *J. Am. Chem. Soc.*, **73**, 4574 (1951).
(16) (a) G. K. Radda, *Curr. Top. Bioenerg.*, **4**, 81 (1971); (b) L. Brand and J. R. Gohlke, *Annu. Rev. Biochem.*, **41**, 843 (1972); (c) G. M. Edelman and W. D. McClure, *Acc. Chem. Res.*, **1**, 65 (1968); (d) A. S. Wagonner and L. Styrer, *Proc. Natl. Acad. Sci. U.S.A.*, **67**, 519 (1970); (e) D. C. Turner and L. Brand, *Biochemistry*, **7**, 338 (1968).
(17) E. M. Kosower, H. Dodiuk, K. Tanizawa, M. Ottolenghi, and N. Orbach, *J. Am. Chem. Soc.*, **97**, 2167 (1975).
(18) E. M. Kosower, "An Introduction to Physical Organic Chemistry", Wiley, New York, N.Y., 1968.
(19) (a) M. Arshadi, R. Yamdagni, and P. Kebarle, *J. Phys. Chem.*, **74**, 1475 (1970); (b) I. Dzidic and P. Kebarle, *ibid.*, **74**, 1466 (1970).
(20) (a) E. Döller, *Z. Phys. Chem. (Frankfurt am Main)*, **31**, 274 (1962); (b) J. R. Brockelhurst, R. B. Freedman, D. J. Hancock, and G. K. Radda, *Biochem. J.* **116**, 721 (1970); (c) M. Grätzel, K. Kalyanasundaram, and J. K. Thomas, *J. Am. Chem. Soc.*, **96**, 7869 (1974).